Design of a Submarine 30-km MgB2 Cable for the Combined Transfer of 0.3 GWe and LH2 from Offshore Plants to the Ravenna Port

Design of a Submarine 30-km MgB_2 Cable for the Combined Transfer of 0.3 GW_e and LH_2 from Offshore Plants to the Ravenna Port

Michela Bracco, Alessandro Balbo, Christian-Erik Bruzek, Marco Breschi, *Senior Member, IEEE*, Lorenzo Cavallucci, *Member, IEEE*, Stefania Farinon, Antonio Macchiagodena, Giovanni Mangiulli, Riccardo Musenich, Luca Soldati, and Laura Savoldi, *Member, IEEE*

***Abstract*—A submarine, hybrid cable for the simultaneous transfer of green electricity and Liquid Hydrogen (LH_2) in a 30 km-long pipeline from an offshore renewable power plant, in the Adriatic Sea is presented here. The superconducting (SC) cable is designed with MgB_2 strands to carry the transport current with a significant margin. The SC strands are twisted around a bundle of normal conducting strands with the function of protecting against overcurrents and ensuring at the same time flexibility of the cable. The SC cable, covered by multiple layers of cold dielectric, is inserted into a corrugated pipe, constituting the inner part of a cryostat where LH_2 flows. LH_2 has the dual function of cryogen and energy carrier. The outer part of the cryostat is designed to limit the heat load to less than 2 W/m, and to withstand the pressure in operation due to the submarine installation at a maximum depth of $\sim$ 50 m.**

***Index Terms*—Energy storage, hydrogen economy, MgB_2 wires and tapes, power cables.**

Received 25 September 2024; revised 19 December 2024; accepted 4 January 2025. Date of publication 13 January 2025; date of current version 4 February 2025. This work was supported in part by the PNRR_IRIS project of INFN through the Italian Ministry of Research and in part by the Ministero dell'Università e della Ricerca through the PRIN 2022 program under Grant D.D.104 -02/02/2022. *(All authors contributed equally to this work.) (Corresponding author: Michela Bracco.)*

Michela Bracco is with the Dipartimento Energia "Galileo Ferraris", Politecnico di Torino, I-10138 Torino, Italy, also with the Istituto Nazionale di Fisica Nucleare, I-16146 Genova, Italy, and also with the Department of Physics, Università degli Studi di Genova, I-16146 Genova, Italy (e-mail: michela.bracco@ge.infn.it).

Alessandro Balbo and Giovanni Mangiulli are with the Dipartimento Energia "Galileo Ferraris", Politecnico di Torino, I-10138 Torino, Italy (e-mail: alessandro.balbo@polito.it; giovanni.mangiulli@polito.it).

Christian-Erik Bruzek is with ASG Superconductors, I-16152 Genoa, Italy (e-mail: bruzek.christian-eric@as-g.it).

Marco Breschi, Lorenzo Cavallucci, and Antonio Macchiagodena are with the Department of Electrical, Electronic and Information Engineering, Università degli Studi di Bologna, I-40126 Bologna, Italy (e-mail: marco.breschi@unibo.it; lorenzo.cavallucci@unibo.it; antoni.macchiagoden2@unibo.it).

Stefania Farinon and Riccardo Musenich are with the Istituto Nazionale di Fisica Nucleare,, I-16146 Genova, Italy (e-mail: stefania.farinon@ge.infn.it; riccardo.musenich@ge.infn.it).

Luca Soldati is with the Department of Physics, Università degli Studi di Genova, I-16146 Genova, Italy (e-mail: luca.soldati5@studio.unibo.it).

Laura Savoldi is with the Dipartimento Energia "Galileo Ferraris", Politecnico di Torino, I-10138 Torino, Italy, and also with the Istituto Nazionale di Fisica Nucleare, I-16146 Genova, Italy (e-mail: laura.savoldi@polito.it).

Color versions of one or more figures in this article are available at https://doi.org/10.1109/TASC.2025.3528923.

Digital Object Identifier 10.1109/TASC.2025.3528923

I. Introduction

In the framework of the transition to a green economy, where hydrogen is anticipated to play a significant role alongside electricity from renewable plants, new wind and solar plants are being designed off the coast of Romagna, Italy, in the Adriatic Sea [1]. A wind farm of 200 MWe and a solar photovoltaic floating plant of 100 MWe, foreseen at a distance of $\sim$ 22 km from the coast, and a wind farm of 400 MWe, planned at $\sim$ 26 km from the coast, have been recently authorized and will be built in the near future. In perspective, the renewable power plants should be combined to a series of electrolyzers with the capability to produce hydrogen up to 4000 tons/year. In the case of off-shore electrolyzers, the transfer to the mainland of the electric and chemical energy via liquid hydrogen (LH_2) cooled superconducting (SC) cables is particularly appealing. Indeed, such a solution allows limiting both the voltage and Joule dissipation. Moreover, the hydrogen is transferred with its maximum energy density. For this case study, the design of a SC power cable for the simultaneous transfer of the green electricity and LH_2, is presented, as part of an Italian High-Relevance National Project, as an alternative to the conventional power cables and pipeline for the transfer of electricity and hydrogen to the mainland, presently foreseen for the case at hand. Hybrid pipelines for the combined transport of electricity through SC materials and hydrogen, deployed as a cryogen for the cooling of the SC, are currently under investigation by several research teams worldwide. In China, for instance, a similar cable is envisaged in [2], while a 100 MW hybrid energy transmission pipeline is under consideration for the future railway systems which will be likely to need both the electricity and hydrogen [3]. In Europe, the H2020 SCARLET Project [4] Consortium is developing, manufacturing and testing a 500 MW DC single-pole 20 kA cable, cooled by LH2 for onshore and offshore applications [5]. A preliminary design of a pipeline, aiming at understanding the range of possible lengths, duct size and cryogen flow for a 1 GW cable was recently presented in [6], which paved the way for the study presented here.

Here, the hybrid pipeline is designed with a single 30-km long magnesium diboride (MgB_2) DC cable inserted into a cryostat, acting as a single pole, inserted in a configuration where the redundancy is achieved by a copper line in parallel, see Fig. 1,

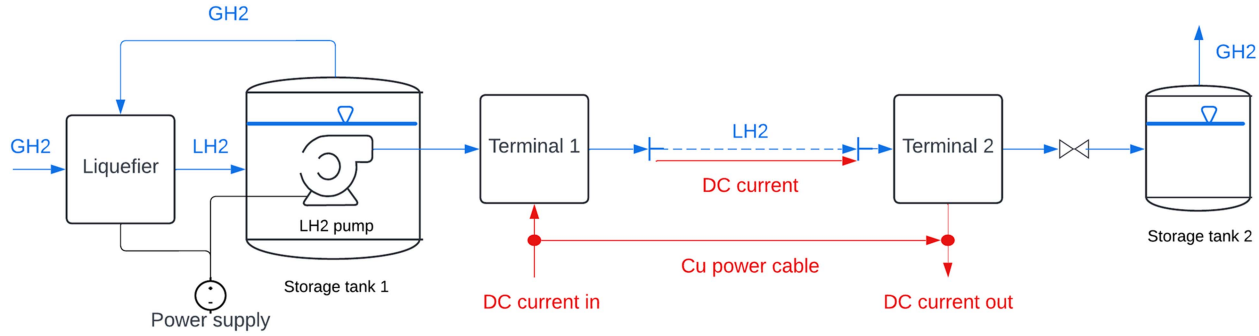

Fig. 1. Layout of the hybrid pipeline, with the auxiliaries for the supply and manage of the cryogen.

described in Section II. In Section III, the layout of the cable is presented and discussed, while the sizing of the pipeline is presented in Section IV, aiming at identifying the operating conditions that would allow the operation of the SC cable in its design conditions. The thermo-mechanical analysis of the pipe and cryostat is then presented in Section V.

II. Layout of Hybrid Line

The scheme of the hybrid power transmission line is shown in Fig. 1: the gaseous hydrogen generated by the electrolyzers is liquefied and transferred to a storage tank at pressure slightly higher than atmospheric. A cryogenic pump has the function to pressurize and send the hydrogen to the line. In order to keep the pressurized liquid at 20 K, the pump and the next heat exchanger are immersed in saturated liquid hydrogen. The hybrid line starts from the termination where gas cooled current leads conduct the current from the room temperature bus bars to the superconducting cable and where a suitable connection inserts the cable into the LH_2 pipeline. A similar termination box is present at the end of the line. The pressurized liquid is then expanded through a throttle valve and sent to a storage tank. Then, the liquid can be gasified and conveyed to the users.

Note that in the storage tank at the pipeline outlet, where the LH_2 is in thermodynamic equilibrium with its vapor, is connected to the pipeline through a lamination valve, where an (ideally) iso-enthalpic expansion of the cryogen is allowed. As in weakly subcooled fluid the iso-enthalpic processes roughly match iso-thermal processes, the control of the saturation temperature of the bath ensures the capability to control the outlet temperature of the pipeline, which is one of the constraints of the pipeline design, see Section IV.

III. Design of Cable Layout

A. Layout

The conductor is based on magnesium diboride wires cabled around a bundle of well-conductive metal wires (copper or aluminum) having the function of protecting the cable against over-current. MgB_2 is an excellent superconductor for low magnetic field applications due to its high critical temperature (39 K), its relatively low cost with respect to other high temperature superconductors and to the availability of wires lengths of several kilometers. To transport electric energy, MgB_2 cables at temperatures higher than 20 K can be used, as demonstrated by the superconducting links assembled and tested at CERN [7]. The cable design starts from the MgB_2 wires produced by ASG Superconductors (Genova, Italy), which do not require any heat treatment [8].

TABLE I
Design Parameters

# MgB_2-wires	42
MgB_2-wire radius	0.67 mm
former radius	8.2 mm
insultation thickness (PPLP)	2.5 mm
MgB_2-wire current	238 A
MgB_2-wire critical current (0.6 T, 29 K)	264 A
I/Ic ratio (0.6 T, 29 K)	0.9

The SC cable, whose design parameters are shown in Table I, is designed to operate under DC conditions at 30 kV and 10 kA with rating electric power of 300 MW. It can operate up to a temperature of 29 K with an I/I_c ratio of 90% . More details about the temperature and magnetic field dependence of the critical current parametrization can be found in [9]. In total, 42-MgB_2 wires are arranged around a copper former with a diameter of 8.2 mm, see Fig. 2(a). The former is designed to be able to allocate the MgB_2 wires. The electrical insulation is provided by polypropylene laminated paper (PPLP) with an overall thickness of 2.5 mm, computed as in (1):

$$t_{ins} = k \cdot R_{in} \left(e^{\Delta V / E_b R_{in}} - 1 \right) \tag{1}$$

where R_{in} is the inner radius of the insultation, ΔV is the voltage across the insulation, E_b is the dielectric strength of the PPLP, and k the safety factor. The resulting electric field and voltage profile are shown in Fig. 2(b).

The insulation thickness is calculated following a conservative approach that neglects the dielectric properties of liquid hydrogen. This assumption is based on the fact that pressurized liquid hydrogen suppresses bubble formation, which increases the LH_2 dielectric strength. The dielectric strength of liquid hydrogen [10] is higher than that of PPLP [11], [12].

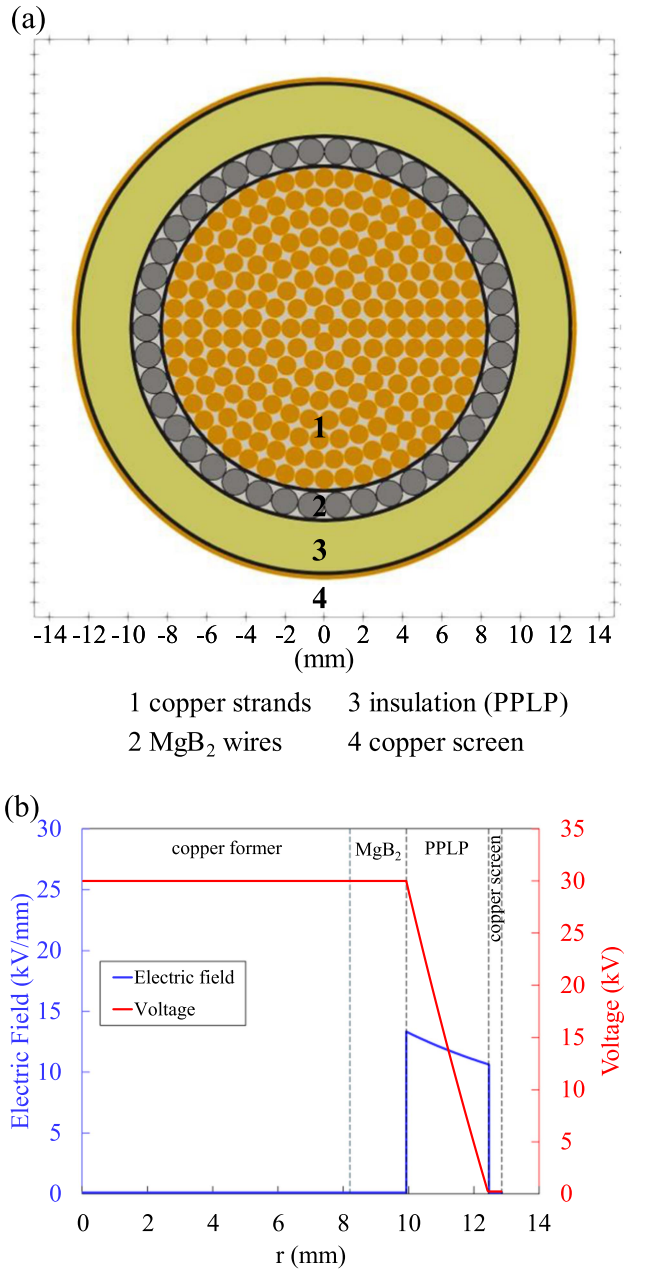

Fig. 2. (a) MgB_2 cable cross section. (b) Decay of the electric field along the thickness of the PPLP layer.

Several semiconductive layers, each with a thickness of less than 1 mm, are interposed between the copper former and the MgB_2-wires as well as between them and the insulation layer to avoid local electric charges deposition. A thin copper screen is grounded to null electric potential. The diameter of the cross-section of the SC cable D_{cable}, up to the copper screen, is 2.6 cm.

B. Losses

A numerical anisotropic electrodynamic model accounting for the non-linear ferromagnetic properties of Nickel and Monel matrix in the MgB_2 wires [13], [14] is applied to preliminary estimate the AC losses due to the current ripple generated by the AC/DC converter. The computed losses, in the order of $\sim$ mW/m, are orders of magnitude lower than other thermal loads and are thus neglected in the sizing of the pipeline in Section III.

IV. Design of Pipeline Layout

The SC cable in the proposed design is inserted in a corrugated pipe, acting as the inner part of a cryostat, in turn inserted into an outer corrugated pipe (outer part of the cryostat). The inner corrugate is thermally insulated from the outer one by layers of low-conductivity insulation and by vacuum and is kept in place by helical low-conductivity spacers. The diameters of the inner and outer corrugates are taken from available commercial pipes. After a first screening, the choice for the inner cryostat was shortlisted to the inner/outer values $D_{in}/D_{out}$of 126.2/145 mm (D1) or 151.6/171 mm (D2). For the outer corrugated pipe, values higher than 198/220 mm have been selected. Note that the selected values allow to consider the possibility of installation of the pipeline by means of the well-established Reel-lay approach [15]. With that approach, the superconducting cable drawn in the cryostat and the pipeline assembled in one place, spooled on a drum and "simply" unspooled on the ship for the off-shore layout.

A. Constraints

The maximum design temperature (29 K) for the MgB_2 cable presented in Section III becomes the upper bound for the design of the LH_2 pipeline embedding the cable. As the pipeline is typically subject to a parasitic load that causes heating of the cryogen, this temperature is the maximum value allowed at the pipeline outlet T_{out}, as no intermediate re-cooling stations are foreseen along the line. The lower temperature bound for the cryogen, i.e., the inlet temperature T_{in}, is kept here at 20 K, that is justified by the fact that the reservoir of saturated liquid must be moderately pressurized to prevent the risk of air infiltration.

A second constraint is given by the outlet pressure p_{out} of the pipeline. The lower bound for the pressure, setting the pressure at the pipeline outlet, is regulated by the saturation condition of the storage tank at the line outlet, see Fig. 1. In the pressure-enthalpy $(p-h)$ diagram of the para-hydrogen (which constitutes by far the largest fraction of the hydrogen in the temperature range at hand), shown in Fig. 3, the saturation curve sets the pressure in the storage tank at the different possible outlet temperature values of the pipeline. In the case of T_{out} =29 K, for instance, the saturation pressure is ~ 0.7 MPa. If some safety margin ($\sim$ 0.1 MPa) to avoid boiling in the pipeline is adopted, the estimated value of p_{out}, used as the constraint in the pipeline sizing, is $\sim$ 0.8 MPa. Different couples of (T_{out}, p_{out}) values are reported in Fig. 3: if T_{out} decreases, p_{out}decreases as well.

B. Pipeline Thermal-Hydraulic Model

The mass, momentum and energy conservation laws are solved for the non-conservative values velocity, pressure and temperature, to evaluate the operating range of the pipelines. The latter is assessed in terms of mass flow rate $\dot{m}$ and inner

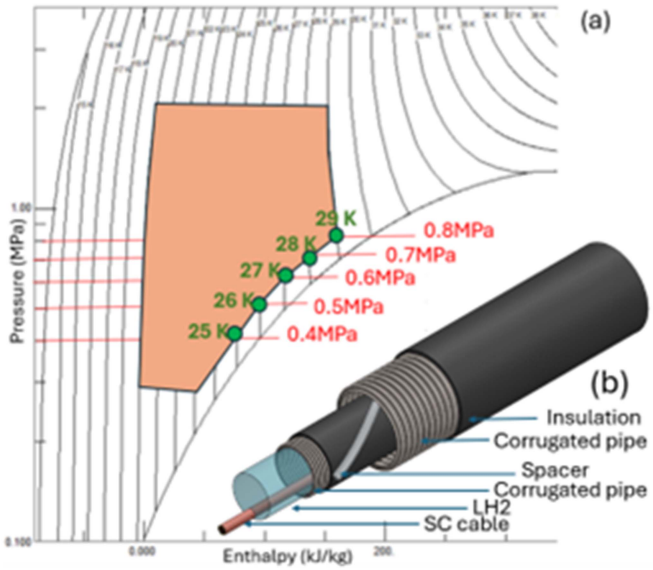

Fig. 3. (a) Pressure-enthalpy diagram for the para-hydrogen in cryogenic conditions, showing parametrically the iso-thermal curves shown down to the saturation (boiling) conditions. (b) Sketch of the hybrid pipeline, with the SC cable lumped in the red cylinder (courtesy of D. Placido).

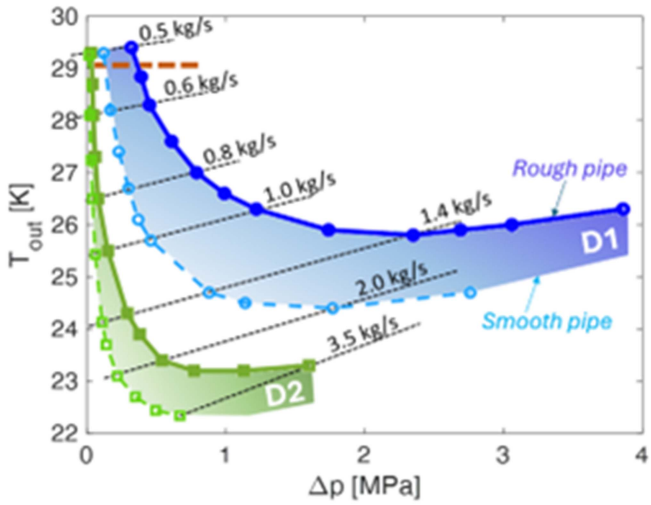

Fig. 4. Operation range for the LH2 pipeline in terms of outlet temperature and pressure drop along the duct. D2 is the corrugated pipe with $D_{in} = 126.2$ mm, D1 the one with $D_{in} = 151.6$mm.

pressure p_{in}, under the set of constraints described above suitably imposed as boundary conditions. Steady state operation is considered, which allows to restrict the simulations to the inner corrugate, the cryogen and the SC cable. The simulations are performed with the OPENSC^2 tool [16], considering the SC cable as a whole object. The thermophysical properties of the coolant are taken from the package Coolprop [17], while the flow section is assumed to be the inner one of the corrugated pipe, as the fluid in the corrugation is taken as stagnant. The friction factor of such pipes is not well known, although for instance the Kauder correlation in [18], so its value has been parametrically varied among two extreme cases, i.e., the value corresponding to a smooth circular pipe (0.01) and the value corresponding to a significant surface roughness in fully turbulent conditions (0.08, already retained in [6]). A steady parasitic load of 2 W/m has been retained in all the simulations. In the simulations, the LH_2 mass flow rate, imposed as one of the boundary conditions, has been parametrically increased from the minimum value that allowed satisfying the constraint on the maximum value of T_{out} with the corresponding value of $p_{out} = 0.8$ MPa to values above which a further increase only affected the pressure drop without any beneficial effect on further decreasing the outlet temperature.

C. LH_2 Operating Range

The results of the simulations are summarized in Fig. 4 for both the size of the inner corrugated pipes and the different friction factors considered in the analysis. The minimum value of $\dot{m}$ that allows the operation below the limit of 29 K is 0.5–0.6 kg/s for all considered cases. A decrease in the parasitic load would be the only viable way to further decrease the value of cryogen mass flow rate needed to keep the SC cable within the design limits.

The curves, obtained for the same duct with a frozen value of the friction factor, show a non-monotonic behavior as the mass flow rate increases. This is expected from the iso-thermal curves in the $(p - h)$ diagram in Fig. 3, as for a given p_{out} an increase in the mass flow rate leads to an increase in the inlet pressure, with a progressive increase of the specific enthalpy h_{in} at 20 K. The given total parasitic load on the pipeline equals in steady state the heat removed by the cryogen as from (2):

$$P_{par} = \dot{m} \times (h_{out} - h_{in}) \tag{2}$$

Beside the increase in the inlet pressure p_{in}, an increase in the flow rate also drives a decrease in the requested enthalpy difference between the outlet and the inlet of the pipeline. For moderate increase in p_{in}, this effect leads to a decrease in T_{out}, but when the increase of h_{in} becomes not negligible, the power balance in (2) can only be accommodated by an increase in the outlet temperature, explaining the non-monotonic behavior in Fig. 3. The presence of a minimum in the curves in Fig. 4 allows identifying the $\dot{m}$ range for which the operation is relevant, i.e., for which the variation of the mass flow rate is directly linked to the decrease of T_{out}.

V. Preliminary Thermo-Mechanical Analysis

The thermo-mechanical analysis relevant for the hybrid pipeline is twofold: along the corrugated pipes, to evaluate the impact of the cryogen pressure on the pipe, and along the cable, to account for the effect of the different thermal contraction of the materials.

The former was performed on the cryostat using an Ansys APDL release 2020 R2 code [19], which is being developed for the superconducting cable. Taking advantage of symmetry, an axisymmetric 2D model of the cross section was created, as shown in Fig. 5, and the adopted element is PLANE183. The

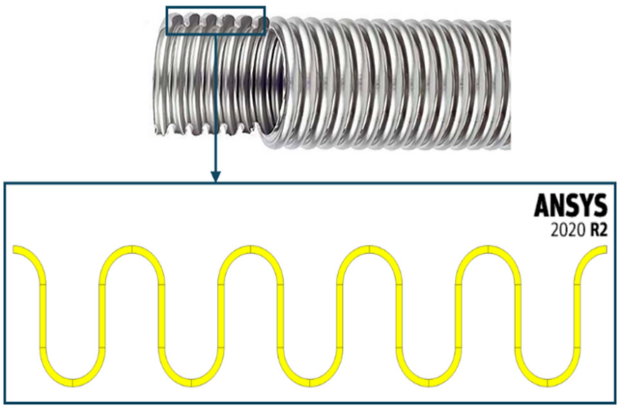

Fig. 5. 2D axial-symmetric model of the transverse section.

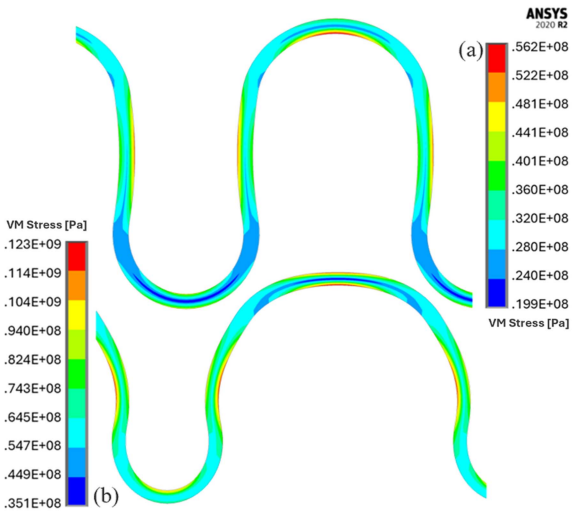

Fig. 6. Von Mises Stress (a) on the outer corrugated tube and (b) on the inner corrugated tube. For both images the deformations are 100 times amplified.

material is a stainless steel, assumed to be elastic, with an elastic modulus of 191 (210) GPa, a stress limit of 350 (1050) MPa, a Poisson's ratio of 0.28 and a thermal contraction coefficient of $2.8{\cdot}10^{-3}$.

To perform the simulation, the nodes at the end of the cryostat have been fixed to account for the fact that the cryostat must have a fixed length. The simulation consists of two steps for the inner corrugated tube and one step for the outer corrugated tube, as listed below:

- For the inner tube:
  - *Step 1*: Cooldown at 20 K since liquid hydrogen flows inside;
  - *Step 2*: Apply a pressure of 10 bar to the inner nodes and of 10^{-5} bar to the outer nodes to simulate the internal pressure due to liquid hydrogen and the vacuum condition on the outside.
- For the outer tube:
  - *Step 1*: Apply a pressure of 10^{-5} bar to the inner nodes and of 4 bar to the outer ones to simulate the internal vacuum condition and the external pressure due to sea pressure at 40–50 m below sea level. The cooling phase is skipped because this cryostat is kept at room temperature.

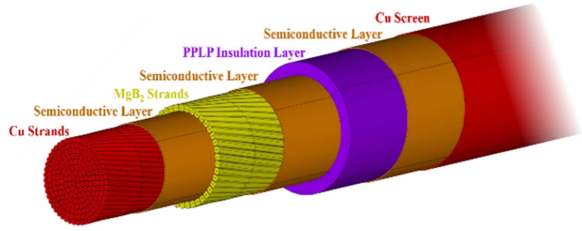

Fig. 7. Geometry of the cable in Ansys APDL.

The results reported in Fig. 6, show that the inner cryostat is much more stressed than the outer one due to thermal contraction. However, on both corrugated tubes, the stresses are low enough for the steel composing the cryostat to withstand them.

As far as the assessment of the thermal contraction is concerned, it can be restricted to the cable, as the corrugated pipe should guarantee the needed compensation for the cryostat. Note that this assessment is also required to determine how long it needs to be made at room temperature so that it reaches the desired length when below 29 K. At the moment, the 3D geometry of the cable shown in Fig. 7 has been defined, and the SOLID186 element has been chosen type for simulations. Since the model is very complex, both mechanically and thermally, the analysis is still under development.

VI. Conclusion

A configuration for a submarine 30-km hybrid pipeline has been proposed and studied in this paper for both electromagnetic, thermal-hydraulic and mechanical points of view, showing encouraging results. While some specific aspects related for instance to the dielectric properties of LH_2 still need to be confirmed by experimental data, the next steps of our project are, for the operating conditions:

- making a more detailed design of the line and of the active auxiliaries, such as current leads and cryogenic pumps;
- carrying out more in-depth thermo-mechanical assessment on the superconducting cable to be sure to cope with the shrinkage at the system boundaries;

The consideration of off-normal conditions such as faults need to be addressed, together with an analysis of the techno-economic competitiveness with respect to different technologies for the separate transfer of power and LH_2.

Acknowledgment

The authors are grateful to Mr. Alberto Bernabini for helpful discussion on the Agnes Project.

References

[1] Accessed: Sep. 16, 2024. [Online]. Available: https://www.agnespower.com/

[2] J. Yang et al., "Roadmap to offshore power-liquid hydrogen co-production and hybrid delivery system based," in *Proc. 15th Int. Conf. Appl. Energy*, Doha, Qatar, Dec. 2023, pp. 1–7, doi: 10.46855/energy-proceedings-10965.
[3] L. Fu et al., "Hydrogen-electricity hybrid energy pipelines for railway transportation: Design and economic evaluation," *Int. J. Hydrogen Energy*, vol. 61, pp. 251–264, Apr. 2024.
[4] N. Magnusson et al., "SCARLET – A European effort to develop HTS and MgB_2 based MVDC cable," *IEEE Trans. Appl. Supercond.*, vol. 34, no. 3, May 2024, Art. no. 5400205, doi: 10.1109/TASC.2023.3340646.
[5] C. E. Bruzek et al., "MgB_2-based MVDC superconducting power cable in liquid hydrogen for hybrid energy distribution," *IEEE Trans. Appl. Supercond.*, vol. 34, no. 3, May 2024, Art. no. 6200405, doi: 10.1109/TASC.2023.3347216.
[6] L. Savoldi et al., "Conceptual design of a SuperConducting Energy Pipeline for LH_2 and power transmission over long distances," *IEEE Trans. Appl. Supercond.*, vol. 34, no. 3, May 2024, Art. no. 5400805.
[7] A. Ballarino, "Development of superconducting links for the large hadron collider machine," *Supercond. Sci. Technol.*, vol. 27, no. 4, 2014, Art. no. 044024.
[8] T. Spina et al., "Recent development and status of ex-situ PIT MgB_2 wires at ASG superconductors," *IEEE Trans. Appl. Supercond.*, vol. 34, no. 3, May 2024, Art. no. 6200304, doi: 10.1109/TASC.2024.3353144.
[9] L. Soldati, M. Breschi, P. L. Ribani, T. Spina, and C.- Bruzek, "AC loss investigation in MgB_2 multifilamentary wires: A numerical study," *IEEE Trans. Appl. Supercond.*, vol. 34, no. 3, May 2024, Art. no. 6200805.
[10] K. N. Mathes, "Dielectric properties of cryogenic liquids," *IEEE Trans. Elect. Insul.*, vol. EI-2, no. 1, pp. 24–32, Apr. 1967.
[11] C. E. Bruzek et al., "MVDC MgB_2 superconducting cables for hybrid power transmission," in *Proc. Jicable'23-11th Int. Conf. Power Insulated Cables*, Lyon, France, Jun. 2023, pp. 1–6.
[12] A. Marian et al., "Validation of the superconducting and insulating components of a high-power HVDC cable," *IEEE Elect. Insul. Mag.*, vol. 34, no. 1, pp. 26–36, Jan./Feb. 2018.
[13] L. Soldati et al., "AC loss investigation in MgB_2 multifilamentary wires: A numerical study," *IEEE Trans. App. Supercond.*, vol. 34, no. 3, May 2024, Art. no. 6200805.
[14] L. Soldati et al., "Analysis of AC losses due to current ripple in MgB_2 wires with helicoidal transformation method," *IEEE Trans. Appl. Supercond.*, early access, Dec. 09, 2024, doi: 10.1109/TASC.2024.3513277.
[15] Offshore Pipe Laying: The Ultimate Guide - OUCO, Accessed: Dec. 15, 2024.
[16] L. Savoldi et al., "Thermal-hydraulic analysis of superconducting cables for energy applications with a novel open object-oriented software: OPENSC2," *Cryogenics*, vol. 124, Jun. 2022, Art. no. 103457.
[17] [Online]. Available: www.coolprop.org
[18] K. Kauder, "Strömungs- und Widerstandsverhalten in gewellten rohren," in *Von Der Fakultät für Maschinenwesen an Der Technischen*, 1971.
[19] ANSYS website. Accessed: Aug. 29, 2024. [Online] Available: https://www.ansys.com/